

# An MHD modeling of high-temperature SiC solution growth

J-M. Dedulle<sup>1,2\*</sup>, F. Mercier<sup>1</sup>, J. Lefebure<sup>1</sup>, D. Chaussende<sup>1</sup>

<sup>1</sup> Laboratoire des Matériaux et du Génie Physique, INP Grenoble - CNRS, 3 parvis Louis Néel, BP 257, 38016 Grenoble, France

<sup>2</sup> IRIS Technologies, 155-157 cours Berriat, 38028 GRENOBLE, France.

\* Corresponding author e-mail: iris.dedulle@wanadoo.fr

**Abstract:** Despite its real advantages compare to seeded sublimation growth, SiC solution growth has never given convincing results. The difficulty of stabilizing the growth front, and thus avoiding any polycrystal formation results from a poor description and understanding of the coupled phenomena that occur in the crucible. This paper addresses the coupled electromagnetism, heat transfer and fluid dynamic modeling of the SiC solution growth process, with special attention being paid to the different convective flows in the liquid. In the first place, it was shown that in the selected configuration, it is possible to simply adjust the temperature gradient in the liquid by precise positioning of the inner crucible with respect to the fixed 'furnace and coil' inductive heating element. Second, three crucible configurations were studied in order to evaluate the impact of the different convective flow mechanisms. It is demonstrated that both Marangoni and electromagnetic convections have to be avoided. The configuration where the flow patterns in front of the crystal are driven only by crystal rotation, insures the most stable growth front. The present paper gives a methodology to create an induction heating modeling with COMSOL Multiphysics<sup>®</sup> and highlight some improvements with the new version v4.0 rather the previous one (v3.5) [1].

**Keywords:** Crystal growth - Liquid phase – Modeling - Induction heating.

## 1. Introduction

Through carbo-reduction of silica sand at high temperature (Acheson process), through vapour-solid or liquid-solid chemical reactions, the formation of SiC is known for more than 50 years [2,3]. However, the growth of SiC single crystals with structural perfection and purity as high as those required by microelectronics applications still is topical. Several decades of

intensive works have not resulted to single crystalline ingots with size and quality equivalent to the most common semiconductors Si, GaAs or InP. To understand this wide gap between easy formation of polycrystalline SiC and the difficult growth of a single crystal, one must consider at least two physical-chemical aspects:

- The Si-C binary phase diagram (see [4] and refs. therein). Due to the peritectic decomposition of SiC at about 2830°C, growth from a stoichiometric melt is not possible at technically relevant system pressures. According to theoretical analysis, such stoichiometric conditions could be obtained for temperatures and pressures exceeding 3200°C and 100 000 atm [4]. At atmospheric pressure, the Liquid-SiC and Vapour-SiC equilibria required for its formation are available only at very high temperature.
- The peculiar crystallography described as polytypism [6-8]. It is well-admitted that the enthalpy of formation difference between the polytypes is very narrow [9], making the stabilization of only one form among all possible very difficult in high temperature processes.

## 2. Multiphysics modelling

### 2.1 Introduction

Experimental approach only has not been sufficient to develop such a process. In the last tenth to fifteenth years, strong improvements have been achieved due to the simultaneous development of modelling and simulation tools as a characterization of the process itself. The macroscopic modelling approach linked with experiments and characterization has allowed to open step by step the black box of the process and to gain insight in the intricate mixture of phenomena. Modelling and simulation of the SiC growth processes, vapour phases routes (PVT,

CVD, M-PVT), are sufficiently mature to be used as a training tool for engineers as well as a growth machine design tool, e.g. when building new process equipment. The key of success would be the combined use of simulation, experiments and characterization in a “daily interaction”. We can use our experience of PVT and CVD modelling in order to develop 3C-SiC single crystal with a liquid phase process (figure 1).

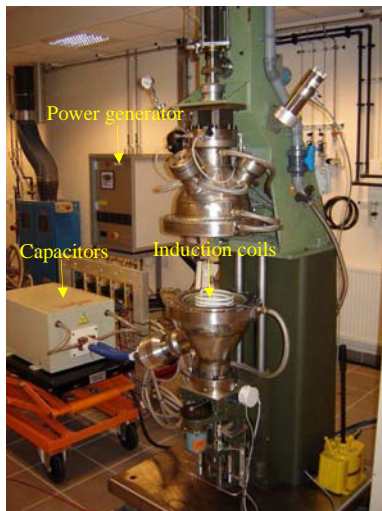
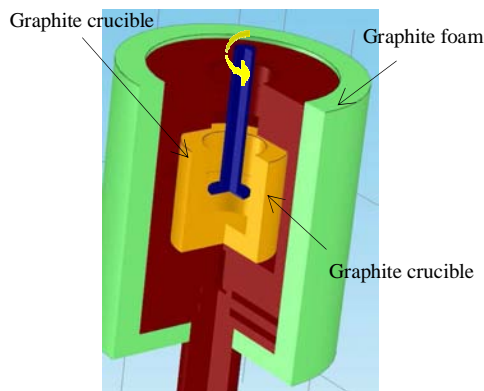


**Figure 1.** SiC crystal growth with liquid phase technique

## 2.2 Model definition for induction heating

Source currents with time dependence induce eddy currents, with respect to Lenz's law, which heat conductive materials by Joule's effect. A complete simulation consists of two successive

steps: first the distribution of the electromagnetic field has to be computed through the full Maxwell equations.

For low frequency ( $f < 1\text{MHz}$ ) the differential equations for the electromagnetic field are derived from Maxwell's equations for the quasi-static approximation. The formulation used by COMSOL Multiphysics in axial symmetry is based on nodal finite element technique. This means that all components are continuous. For this reason we used a vector potential ( $\vec{A}$ ) formulation deduce from  $\text{div} \vec{B} = 0$  equation ( $\vec{B} = \text{rot} \vec{A}$ ), in order to respect the interfaces conditions.

The resultants equations are based on the assumption that the magnetic field is time harmonic with an angular frequency  $\omega$ .

Our reactor, is shaped axisymmetrically (figure 2), thus reducing the magnetic field to a two dimensional problem.

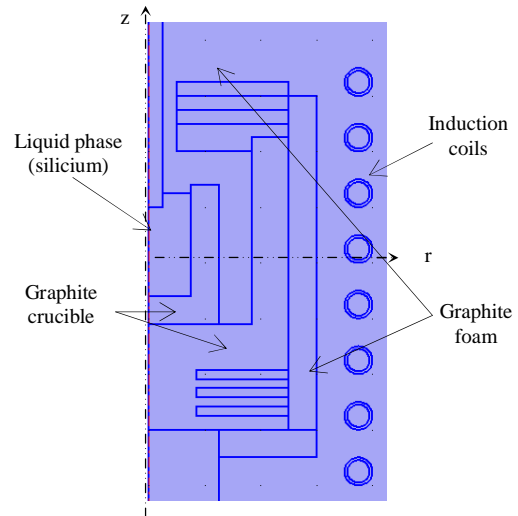


**Figure 2.** The axisymmetric model geometry

Under this assumption, the electric scalar potential is constant on the plane of computation and Coulomb gauge is automatically satisfied. The magnetodynamic equation may be written:

$$\text{rot}(v_r \text{rot} \mathbf{A}) + j\sigma\omega \mathbf{A} + \sigma \nabla \times \mathbf{B} = \mu_0 \mathbf{J}$$

$$\text{with: } \mathbf{A} = \begin{pmatrix} 0 \\ \underline{A}_\phi \\ 0 \end{pmatrix}, \quad \mathbf{J} = \begin{pmatrix} 0 \\ \underline{J}_\phi \\ 0 \end{pmatrix}$$

$\underline{A}_\phi$  : orthoradial component of complex vector potential

$\underline{J}_\phi$  : orthoradial component of complex current density

$J_\phi$  is the total current, eddy current and source current due to supply voltage in each turn coil:

$$J_\phi = -j\sigma\omega A_\phi + \sigma \text{grad}V$$

The 2<sup>nd</sup>e term is a ddp per turn coil. These ddp is different for each turn ( $V_i$ ). But due to the geometry of the coil, the total current in each turns coil is the same ( $I_0$ ). With COMSOL multiphysics v4.0 (single turn domain feature), it is not necessary to impose multiple constraint for an integral property, like the total current for each turn coil  $i$  :

$$I_{\theta_i} = \int_{S_i} \left( -j\sigma\omega A_\theta + \sigma \text{grad}V \right) dS_i = I_0$$

The ddp for each turn using an additional algebraic equation which constrains the total integrated current to be equal to the current value  $I_0$  which you have specified.

At the end of the resolution, we obtained automatically the ddp  $V_i$  (named  $V_{tot\_i}$ ) for each turn, with respect to the constraint  $I_i=I_0$  (for example with 4 turns coil : figure 3).

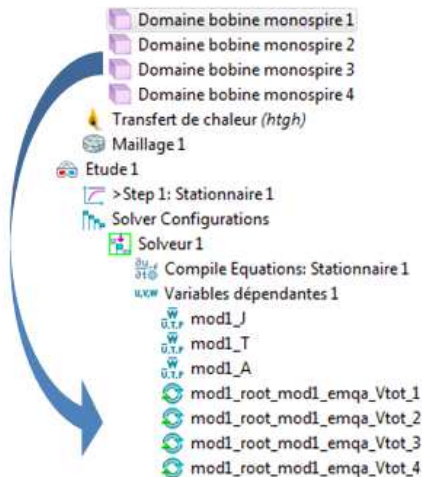


Figure 3. Single turn domain and dependent variables

A set of boundary condition must be formulated for the magnetic model. We imposed zero vector

potential (magnetic insulation) on the limiting box automatically detected by version 4.0. Because of the axisymmetric shape of the reactor, a zero normal induction field is imposed along the symmetry axis (axial symmetry). The version 4.0 automatically detected the set of boundaries along the axial symmetry.

After computation, it's possible to obtain the parameters of the equivalent circuit resistance and inductance (figure 4). The capacity is deduce in order to supply by the capacitors all reactive losses for the inductance (figure 4).

Variables	
Name	Expression
ddp	mod1.emqa.Vtot_1+mod1....tot_3+mod1.emqa.Vtot_4
L	emqa.Lc_1+emqa.Lc_2+emqa.Lc_3+emqa.Lc_4
R	real((ddp)/I0)
C	1/(L*emqa.omega^2)
P_active	R*I0^2/2

Figure 4. Computation of electric parameters

Numerical modelling allows adjusting the temperature and the temperature difference along the crucible by the control of the current in the coil, by adjusting the position of the coil and by modifying geometry.

The phenomena involved in the growth of SiC bulk growth are:

- i) Thermal radiation, induction heating
- ii) Siliconium fluid transport
- iii) Liquid and surface chemistry

In this paper we treat induction heating and liquid phase siliconium fluid transport. The energy equation describes the temperature field and the heat transfer in the reactor.

In the energy equation, the major assumptions are:

1. The Dufour effect, causing an energy flux as a result of concentration gradients is neglected,
2. Interdiffusion of the chemical species is neglected,
3. Heat production/destruction due to chemical reactions in the gas mixture is neglected,
4. Steady state is obtained during crystal growth process.

Under these assumptions, the governing equation for thermal energy may be written:

$$-\text{div}(k\text{grad}T) + \rho C_p \mathbf{v} \cdot \text{grad}(T) = Q_{\text{th}}$$

- T: temperature
- k: thermal conductivity
- $\mathbf{v}$  : velocity of fluid
- C<sub>p</sub> : heat capacity
- Q<sub>th</sub>: Joule losses density

A set of boundary conditions must be formulated for the thermal problem (figure 5):

- (i): zero-temperature gradients normal to the symmetry axis
- (ii): Thermal flux boundary conditions relative to the advective and radiative phenomena are fixed for the reactor lateral, top and bottom graphite foam (figure 5 - blue):

$$-k\text{grad}T \cdot \mathbf{n} = h(T - T_{\text{amb}}) + \sigma_s \varepsilon (T^4 - T_{\text{amb}}^4)$$

- h: advection coefficient (W.m<sup>-2</sup>.K<sup>-1</sup>)
- T<sub>amb</sub>: ambient temperature (K)
- σ: Stefan-Boltzmann's constant (W.m<sup>-2</sup>.K<sup>-4</sup>)
- ε: emissivity
- $\mathbf{n}$  : unit normal vector to the wall

- (iii): Thermal flux boundary conditions relative to radiative energy transfer including emission, reflection and adsorption (in axial geometry since v3.5 version of COMSOL Multiphysics). Radiant surfaces are assumed to behave like grey bodies and are characterized by an emissivity (figure 6 – yellow). We also assume that the radiant surfaces are separated by non participating media, i.e. that the gases inside the cavity do not affect radiant energy transfers.

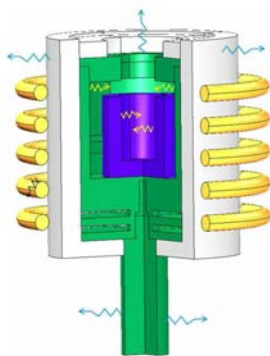


Figure 5. Boundary conditions for thermal model

The Joule losses density (subdomain expression P\_joule) is the source term of energy equation (figure 6).

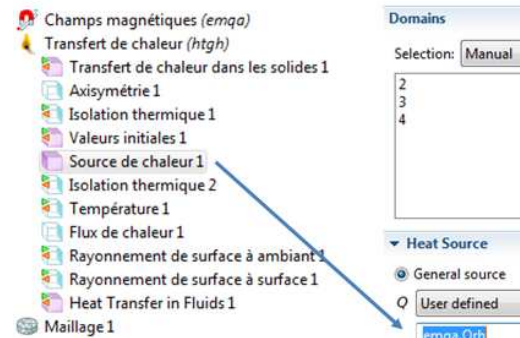


Figure 6. Strategy of resolution : segregated solver

The thermal and electrical physical properties are dependent of the temperature. Due to physical properties, radiative effect and strong coupling model, induction heating is a non linear process. A segregated strategy of computation is used in order to solve the induction heating problem (figure 7).

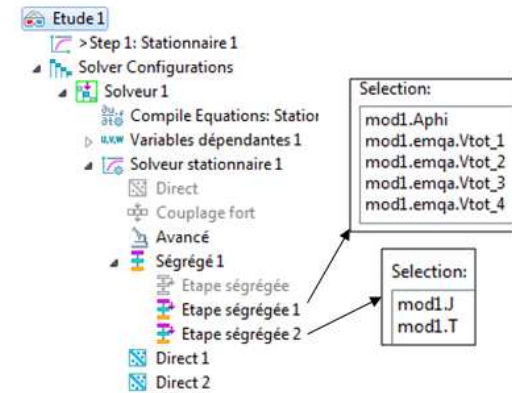


Figure 7. Strategy of resolution : segregated solver

### 2.3 Melt flow model

The flow is described by the Navier-Stokes equations:

$$\nabla \cdot \mathbf{u} = 0$$

$$\rho \frac{\partial \mathbf{u}}{\partial t} + \rho(\mathbf{u} \cdot \nabla)\mathbf{u} = \nabla \cdot \left[ -p\mathbf{I} + \eta(\nabla\mathbf{u} + (\nabla\mathbf{u})^T) \right] + \mathbf{F}$$

In these equations,  $u$  denotes the velocity,  $\rho$  the density,  $\eta$  the dynamic viscosity, and  $p$  the pressure (Pa). For the hydrodynamic problem,  $\frac{L}{D} \leq 0.7$ , where  $\frac{L}{D}$  is the aspect ratio of the liquid with  $L$ , height of liquid and  $D$ , diameter of fluid cylinder. In this case, convection flow can be considered as axisymmetric.

To simplify the complex convection phenomena, melt flow is divided into three main contributions: buoyancy convection, forced convection, electromagnetic convection and Marangoni convection. The computational domain used for 2D-axisymmetry simulation is shown in figure 8.

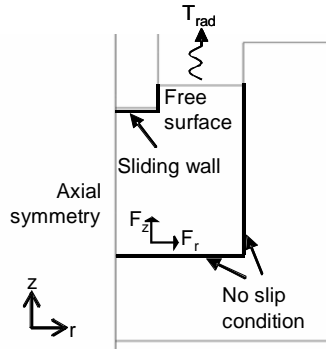


**Figure 8.** Boundary conditions for melt flow model

For volume forces acting in the melt, axial contribution has two components, electromagnetic force density,  $F_{Z_{EM}}$  and buoyancy force density  $F_{Z_{Buo}}$  :

$$F_z = F_{Z_{EM}} + F_{Z_{Buo}}$$

$$\text{with } F_{Z_{EM}} = -\frac{1}{2} \text{real}(j_0 b_r^*)$$

$$\text{and } F_{Z_{Buo}} = \alpha \cdot g \cdot \rho \cdot (T - T_0)$$

The radial contribution of volume force density is only due to electromagnetic forces:

$$F_r = \frac{1}{2} \text{real}(j_0 b_z^*)$$

Rotation of crystal is taken into account by introducing a sliding wall for boundary settings. The velocity components in the plane are zero, and that in the angular direction is equal to the

angular velocity,  $\omega$ , times the radius,  $r$ :  
 $w_w = \omega_{cruc} \cdot r$

Marangoni convection occurs when the surface tension of an interface, in this case the liquid-gas interface, depends on the temperature distribution due to the radial thermal gradient. Surface tension ( $\gamma$ ) is temperature-dependent:

$$\gamma(T) = \gamma_0 + \chi(T - T_0)$$

where  $\chi$  is the temperature derivative of the surface tension, also called the Marangoni coefficient. The equation describes the forces that the Marangoni effect induces on the interface (liquid/gas):

$$\mathbf{n} \cdot \boldsymbol{\tau} \cdot \mathbf{s} = \frac{\partial \gamma}{\partial s} = \chi \frac{\partial T}{\partial s}$$

where  $\boldsymbol{\tau}$  is the viscous stress tensor and  $s$  is a unit vector along the tangent interface.

This equation states that the shear stress ( $\mathbf{n} \cdot \boldsymbol{\tau} \cdot \mathbf{s}$ ) on a surface is proportional to the temperature gradient, which can be written as follows in the case of a flat horizontal interface:

$$\eta \frac{\partial u}{\partial z} = \chi \frac{\partial T}{\partial r}$$

where  $u$  is the radial velocity.

To impose the condition that the shear stress is proportional to the temperature gradient on the free surface, we used a weak contribution feature in the Laminar Flow interface to add the weak term:

$$\text{test}(u) \cdot \chi \frac{\partial T}{\partial r}$$

$\text{test}(u)$  is the test function for velocity along the radius axis.

This term replace the condition on the  $r$ -velocity from the slip boundary condition in the laminar flow interface. With the version 4.0 is much more simpler, it's not necessary to define a new set of weak form equation and introduce a Lagrange multiplier.

At the boundaries representing the cylinder surface a No slip condition applies (figure 6), stating that all velocity components equal zero. At the rotation axis, the radial velocity is set to zero. This condition allows flow in the tangential direction of the boundary but not in the normal direction. The surface of the liquid is assumed to be flat.

### 3. Results

As a first step, in a previous work it was shown [1] that in the selected configuration, it is possible to simply adjust the temperature gradient in the liquid by precise positioning of the inner crucible with respect to the fixed ‘furnace and coil’ inductive heating element.

Three crucible configurations were studied (figures 9 and 10) in order to evaluate the impact of the different convective flow mechanisms (figure 11).

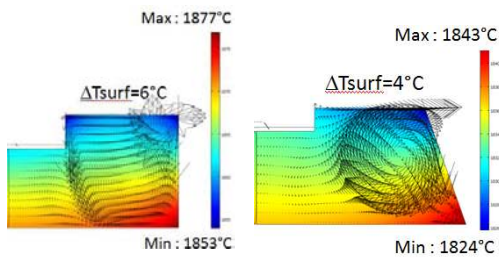


Figure 9. Evaluation of three configurations

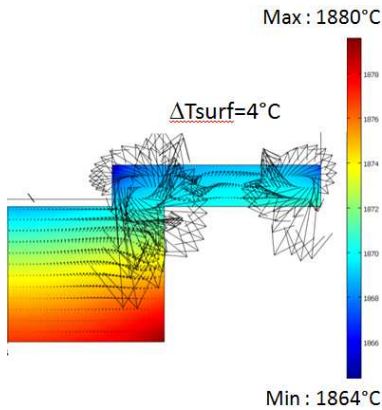


Figure 10. Podium crucible design

	Cylindrical crucible (h <sub>S</sub> =1 cm)	Cylindrical crucible (h <sub>S</sub> =3 cm)	Tipped crucible	Podium crucible
Growth rate	B	B	C	A
Convection control	B	C	B	A
Stability of growth front	A	C	A	A
Process stability	B	C	A	A
Duration of typical run	10 hours	< 5 hours	> 10 hours	>25 hours

Figure 11. Evaluation of three configurations

The podium crucible design (figure 10), in which the global flow pattern is driven mainly by the crystal rotation, is the most appropriate geometry as it enabled a 3C-SiC wafer to be grown with a stable process, a stable growth front at a growth rate of up to 65 μm/h.

### 4. Conclusions

The importance of Marangoni and electromagnetic convections in destabilizing the solution growth process was demonstrated.

The SiC solution growth process could be an alternative to sublimation, particularly for the growth of ‘low-temperature polytypes’ like 3C-SiC.

### 5. References

1. J-M Dedulle, F. Mercier, D. Chaussende and M. Pons, Modeling of 3C-SiC Single Crystal Growth, Conference COMSOL 2007, Paris.
2. O'Connor J. R., in *The Art and Science of Growing Crystals*, edited by J. J. Gilman (John Wiley & Sons, New York, 1963), p. 93-118.
3. Knippenberg W. F., *Philips Research Reports* 1963, **18**, 161-273.
4. Rocabois P., Chatillon, C., and Bernard, C., *High Temperatures - High Pressures* 1996, **27/28**, 3-23.
5. Tsvetkov V. F., Allen, S. T., Kong, H. S., and Carter, C. H., Jr., *Institute of Physics Conference Series* 1996, **142**, 17-22.
6. Gomes de Mesquita A. H., *Philips Technical Review* 1969, **30**, 36-47.
7. Jagodzinski H., *Acta Cryst.* 1954, **7**, 300.
8. Verma A. R., *Journal of Scientific & Industrial Research* 1966, **25**, 487-9.
9. Tairov Y. M. and Tsvetkov, V. F., *Progress in Crystal Growth and Characterization* 1983, **7**, 111-62.